



MR AXEL TJÖRNSTRAND (Orcid ID : 0000-0002-5622-7744)

DR OSKAR RAGNARSSON (Orcid ID : 0000-0003-0204-9492)

Article type : Original Article

Pre- and postoperative ^{68}Ga -DOTATOC positron emission tomography for hormone-secreting pituitary neuroendocrine tumors

Running title: ^{68}Ga -DOTATOC PET in functioning PitNETs

Authors: Axel Tjörnstrand^{1,2} | Olivera Casar-Borota^{3,4} | Kerstin Heurling^{5,6,7} | Michael Schöll^{5,6,8} | Peter Gjerdtsson^{9,10} | Oskar Ragnarsson^{1,11} | Helena Filipsson Nyström^{1,5,11}

Affiliations:

¹Department of Internal Medicine and Clinical Nutrition, Institute of Medicine, Sahlgrenska Academy, University of Gothenburg, Göteborg, Sweden

²Department of Radiology, Sahlgrenska University Hospital, Göteborg, Sweden

³Department of Immunology, Genetics and Pathology, Uppsala University, Uppsala, Sweden

⁴Department of Clinical Pathology, Uppsala University Hospital, Uppsala, Sweden

⁵Wallenberg Centre for Molecular and Translational Medicine, Sahlgrenska University Hospital, Göteborg, Sweden

⁶Institute of Neuroscience and Physiology, Department of Psychiatry and Neurochemistry, University of Gothenburg, Göteborg, Sweden

⁷Antaros Medical, Mölndal, Sweden

⁸Dementia Research Centre, Queen Square Institute of Neurology, University College London, United Kingdom

⁹Department of Clinical Physiology, Sahlgrenska University Hospital, Göteborg, Sweden

This article has been accepted for publication and undergone full peer review but has not been through the copyediting, typesetting, pagination and proofreading process, which may lead to differences between this version and the [Version of Record](#). Please cite this article as [doi: 10.1111/CEN.14425](https://doi.org/10.1111/CEN.14425)

This article is protected by copyright. All rights reserved

¹⁰Department of Molecular and Clinical Medicine, Institute of Medicine Sahlgrenska Academy, University of Gothenburg, Göteborg, Sweden

¹¹Department of Endocrinology, Sahlgrenska University Hospital, Göteborg, Sweden

Correspondence: Axel Tjörnstrand, Department of Radiology Sahlgrenska University Hospital, Bruna Stråket 11 B, Sahlgrenska University Hospital, SE-413 45 Göteborg, Sweden; Email: axel.tjornstrand@vgregion.se; Phone: +46-313426861

Article type: Original article

Abstract length: 288 words

Text length: 3696 words

No. of graphics: 8 (3 tables, 5 figures)

No. of references: 22

ACKNOWLEDGEMENTS

To all colleagues that have provided contact with patients, especially Ass Prof Bertil Ekman, Department of Endocrinology, University hospital in Linköping, Sweden as well as to all patients who gave their consent, making this study possible. A special thanks for the great work goes to co-workers at Sahlgrenska University hospital, Gothenburg, Sweden Jakob Himmelman (clinical physicist) and Oleksiy Itsenko (radiochemist) at Department of Nuclear Medicine for tracer synthesis and imaging acquisition, senior consultant Doerthe Zieglitz, MD, Department of Radiology for the postsurgical MRI evaluation, to the biomedical analysts, and to nurse Lena Kullin at Department of Endocrinology, for managing and logistics of patients and controls for this study. Also a special thanks to Tor Halle at the Uppsala University Hospital, Uppsala, Sweden for his technical assistance in the immunohistochemical analyses.

CONFLICT OF INTEREST

The authors declare that they have no conflict of interest that could be perceived as prejudicing the impartiality of the research reported.

FUNDING INFORMATION

The study was financed by grants from the Swedish state under the agreement between the Swedish government and the county councils, the ALF-agreement (ALFGBG-717311), the Healthcare Board, Region Västra Götaland (Hälsö- och sjukvårdsstyrelsen), Novo Nordisk foundation, Wilhelm and Martina Lundgren Fund, and the Swedish Medical Society, the Anna-Lisa and Bror Björnsson grant, the Gothenburg Medical Society and the Royal Society of Art and Science in Gothenburg. Olivera Casar-Borota was supported by the Swedish Cancer Society (grant number 190157 Fk) and by the grant from the Swedish state under the agreement between the Swedish government and the county councils (ALF-agreement).

AUTHOR CONTRIBUTION

All authors contributed significantly to the work, meet the criteria for authorship, provided critical review of the manuscript and approved the final version.

DATA AVAILABILITY STATEMENT

The data that support the findings of this study are available from the corresponding author upon request.

ORCID

Axel Tjörnstrand: <https://orcid.org/0000-0002-5622-7744>

Olivera Casar-Borota: <https://orcid.org/0000-0001-7376-7331>

Kerstin Heurling: <https://orcid.org/0000-0001-8497-9612>

Michael Schöll <https://orcid.org/0000-0001-7800-1781>

Peter Gjertsson: <https://orcid.org/0000-0001-5643-3882>

Oskar Ragnarsson: <https://orcid.org/0000-0003-0204-9492>

Helena Filipsson Nyström: <https://orcid.org/0000-0002-4670-3401>

Abstract

Objectives: Somatostatin receptors (SSTRs) are potential targets for detecting pituitary neuroendocrine tumors (PitNETs) that can be visualized effectively with ^{68}Ga -labeled PET tracers. With this study, we have evaluated the diagnostic properties of such a tracer, ^{68}Ga -DOTATOC, in patients with hormone-producing PitNETs before and after surgery.

Design/Methods: This prospective case-control study presents preoperative positron emission tomography (PET) and histopathological data in 18 patients with somatotroph (n = 8), corticotroph (n = 7), and thyrotroph (n = 3) PitNETs. Patients were scanned pre- and postoperatively with ^{68}Ga -DOTATOC PET. For the postoperative part of the study, patients with gonadotroph tumors (n = 7) were also included. Fifteen pituitary healthy controls underwent the same protocol once. The maximum standard uptake value (SUV_{max}) was analyzed in manually outlined regions around the tumor in patients and around the pituitary gland in controls. Tumor specimens were collected during surgery in subjects for assessment of adenohypophyseal tumor cell type and the SSTR expression.

Results: Thyrotroph tumors showed higher uptake (median SUV_{max} 41.1; IQR 37.4-60.0) and corticotroph tumors lower uptake (SUV_{max} 6.8; 2.6-9.3) than normal pituitary gland (SUV_{max} 13.8; 12.1-15.5). The uptake in somatotroph tumors (SUV_{max} 15.9; 11.6-19.7) was similar to the uptake in the pituitary gland. There was a strong correlation between SUV_{max} and SSTR2 expression ($r = 0.75$ ($P < .01$)). In the postoperative evaluation, PET was able to correlate tracer uptake with biochemical cure and non-cure in patients with an abnormal postoperative magnetic resonance image and a preoperative tumor uptake $\text{SUV}_{\text{max}} > 13.8$.

Conclusions: ^{68}Ga -DOTATOC PET can be used to detect thyrotroph tumors in the pre- and postoperative imaging assessment. Corticotroph tumors had a significantly lower uptake compared to the pituitary gland but without a distinct increased tumor uptake the clinical postoperative value is limited.

KEYWORDS: DOTATOC PET, pituitary neuroendocrine tumor, somatostatin receptor imaging

1 | INTRODUCTION

Tumors arising from hormone-producing cells in the anterior lobe of the pituitary gland are members of the neuroendocrine family, pituitary neuroendocrine tumors (PitNETs),¹ and can be either functioning, i.e. hormone-producing, or nonfunctioning (NF), i.e. without hormone secretion.² PitNETs are common, representing approximately 10% of all intracranial tumors^{3,4} and account for 25% of all intracranial surgical resections.⁵

Magnetic resonance imaging (MRI) is the "gold standard" for the detection of PitNETs. There are, however, limitations to this technique. MRI has low sensitivity for detection of tumors <5 mm.⁶ With the addition of contrast agent, the detection rate for smaller tumors is improved but, with low specificity, the utility of MRI for small tumors is limited.⁷ Particularly in patients with Cushing's disease, corticotroph tumors manifest frequently as microadenomas (<10 mm) and cannot be detected by MRI in up to 40% of the cases.^{8,9} Another challenge with MRI is postoperative radiological assessment. Many patients with functioning PitNETs undergo surgery, resulting in altered anatomic conditions, postoperative changes, and implant insertion that can cause imaging artifacts. Discrimination of tumor tissue from scar tissue is challenging and, because MRI only provides morphological information, the detection of residual tumor tissue is only possible by observing longitudinal tumor growth on repeated scans. Moreover, the relative lack of functional information limits the evaluation of nonsurgical treatment response.

Positron emission tomography (PET) using ⁶⁸Ga-labeled somatostatin (SSTR) analogs is the molecular imaging modality of choice for the detection of neuroendocrine tumors, for which the defined characteristic is SSTR expression.¹⁰⁻¹² Although PitNETs also express SSTR, this technique has not been properly evaluated for these tumors. Recently, we and others have reported intriguing results from small-scale pilot studies arguing for the diagnostic potential of ⁶⁸Ga-labelled octreotide DOTATOC PET, by demonstrating meaningful differences in tracer uptake between the normal pituitary gland and NF-PitNETs (mostly gonadotroph tumors)¹³ as well as corticotroph tumors.¹⁴ Furthermore, SSTR PET has also found use in the imaging assessment of patients with multiple endocrine neoplasia type 1.¹⁵ However, these pilot studies were only targeted at a subset of PitNETs and, apart from our NF-PitNET study,¹³ the published imaging data were not accompanied by relevant histopathological data.

Our hypothesis was that SSTR expression is different in functioning PitNETs compared to normal pituitary gland and, therefore, tumors can be visualized by using ^{68}Ga -DOTATOC PET. To test the hypothesis, we have conducted a prospective, case-control study, including patients with different PitNET subtypes who have been investigated with ^{68}Ga -DOTATOC PET before and after surgery.

2 | MATERIALS AND METHODS

2.1 | Study design

This prospective, case-control study was conducted at the Departments of Endocrinology and Nuclear Medicine at the Sahlgrenska University Hospital, Gothenburg, Sweden between December 2015 and May 2020. Adult PitNET patients were examined with ^{68}Ga -DOTATOC-PET before and 6-8 months after pituitary surgery. Height and weight were measured before each PET scan. In premenopausal women, a pregnancy test was used to exclude pregnancy. After the PET scan, all subjects filled in a standardized report form to register any possible side effects within 24 hours after tracer administration. Control subjects underwent the same PET protocol once.

The Regional Ethical Review Board (Gothenburg, Sweden) approved the study, which was conducted in accordance with the Declaration of Helsinki. Signed informed consent was obtained from all subjects before engaging in the study protocol, that also allowed for collection of tumor specimens during surgery, after full explanation of the purpose and nature of all procedures used.

2.2 | Subjects

Twenty-three PitNET patients (25-74 years of age at diagnosis; 10 men) were included in this study: two were NF-PitNETs of corticotroph cell origin from a previous publication¹³ and the remaining 21 were somatotroph (n = 9), corticotroph (n = 8), and thyrotroph (n = 4) tumors at clinical presentation. For the postoperative part of the study, seven patients with clinical NF-PitNETs of gonadotroph cell origin were included for their postoperative PET evaluation, where the preoperative PET scan data are presented in a previous pilot study.¹³ The patients, all recruited from university hospitals in Sweden and referred for

Accepted Article

pituitary surgery, were diagnosed in a routine clinical setting based on MRI evidence of a pituitary tumor, biochemical analyses, and clinical presentation that met the criteria for ICD-10 code pituitary tumor (D35.2) in combination with acromegaly (E22.0), Cushing's disease (E24.0), or thyroid-stimulating hormone (TSH) hypersecretion (E05.8). Biochemical analyses performed pre- and postoperatively include, but are not restricted to, S-TSH, S-FT3, S-FT4, S-ACTH, S-cortisol, S-IGF-1, S-LH, S-FSH, S-testosterone, S-estradiol and depending on hormonal presentation oral glucose suppression test, TRH test, T3-suppression test and/ or dexametason suppression test are added. Patients with lactotroph tumors were not included, as they rarely undergo pituitary surgery. In all cases but one, the tumor was seen on the pituitary MRI. Patients without clinical or biochemical signs of pituitary hormone overproduction were deemed as NF-PitNET. For patients with corticotroph tumors <7 mm or without a detectable tumor on MRI, the diagnosis was confirmed by using inferior sinus petrosus catheterization sampling. Patients ≥ 18 years of age with a treatment-naive tumor (including surgery, somatostatin analogues, or dopamine agonists) waiting surgical treatment were recruited for this study.

Sixteen controls (37-79 years of age; 9 men) were included, comprising two groups. The first group included 13 healthy volunteers who were randomly selected from the population registry in Gothenburg, Sweden. Exclusion criteria included any pituitary disease and/or ongoing treatment with somatostatin analogues or dopamine agonists. To be included in the evaluation as a control, the MRI had to be negative for incidentalomas in the pituitary. The second group included three controls with thyroid-associated ophthalmopathy (TAO) who were participating in another study (<http://www.clinicaltrials.gov>; identifier NCT02378298), where ^{68}Ga -DOTATOC PET was performed using the same scanning protocol as in our patients to evaluate eye-muscle inflammation. Inclusion criteria for that study were euthyroid men or women ages 18-70 years with TAO necessitating intravenous glucocorticoid treatment. All controls except two were presented in our previous publication.¹³ ^{68}Ga -DOTATOC PET was performed before any glucocorticoid treatment was administered. Exclusion criteria for TAO controls were the same as those for healthy controls.

Two patients discontinued participation in the study before the first PET scan. One had to undergo pituitary surgery rapidly before the PET scan could be performed and the other chose to withdraw further participation. Two patients with hypercortisolism and a

suspected corticotroph tumor, respectively, were excluded from analyses as explorative surgery was unable to confirm any tumor finding. One patient with clinical hyperthyroidism of central origin declined surgical treatment and was excluded after the first PET scan and is not included in the preoperative analyses. Two patients (#15 and #17; Table 1) with preoperative PET scan and resected tumor specimen for immunohistochemical (IHC) analysis dropped out before postoperative PET scan was performed. Moreover, the postoperative evaluations for three patients (#9, #10, and #14; Table 1) have been delayed because of the Covid-19 pandemic as clinical research visits to the hospital have not been allowed. Consequently, these patients are awaiting their postoperative evaluation. One of the control subjects had a panic attack in the MRI scanner and chose to withdraw further participation.

Thus, in this study, we present preoperative PET and histopathological data from 18 patients as well as PET data from 15 control subjects. Data from the postoperative PET scans, are presented in 20 patients; 13 of 18 patients with preoperative PET and 7 patients with NF-gonadotroph tumors from a previous publication. A flowchart over the inclusion and research visits for patients and controls is presented in the appendix to help with a better overview of the process.

2.3 | MRI

MRI was performed according to the clinical protocol of the Department of Radiology, Sahlgrenska University Hospital, Gothenburg, Sweden, including a T1-weighted scan, both with and without gadolinium contrast enhancement as well as a 3D-acquired T1 sequence. T2 sequences were also used for tumor evaluation. Similar clinical protocols were undertaken at the regional hospitals for patients that were recruited from other regions. If the 3D-acquired T1 sequence was missing, a complementary MRI was carried out at the Department of Radiology, Sahlgrenska University Hospital, Gothenburg, before the PET scan. MRI scans were performed within 3 months of the ^{68}Ga -DOTATOC PET. For controls, MRI scans were performed by the same protocol as for the patients but without any contrast agent.

Post-operative MRI scans were assessed by an experienced neuroradiologist (DZ) with respect to residual tumor tissue and postoperative changes.

2.4 | ⁶⁸Ga-DOTATOC PET

Radiotracer synthesis and quality control were performed with the same scanning protocol as in our previous publication.¹³ Scanning was performed with a dynamic list mode acquisition starting at the time of injection to collect emission data over a 45-minute period. The list mode data were reconstructed into 14 frames (5 × 60, 5 × 180, 3 × 300, and 1 × 600 seconds). All PET images were iteratively reconstructed (MLEM/OSEM) using five iterations and 21 subsets with time-of-flight resolution recovery (TrueX), computed tomography (CT)-based attenuation and scatter corrections, and a 3-mm Gaussian postprocessing filter.

The postsurgical PET scan was performed with the same study protocol ≥6 months after pituitary surgery to avoid any interference in uptake due to inflammatory activity.

2.5 | Image analysis

PMOD software v3.8 (PMOD Technologies, Ltd.) was used for image analysis. MRI and PET images were co-registered using the "Fuse it" toolkit. The PET-images were motion corrected by aligning all frames to a reference frame created by the mean position of the first three frames using the "motion correction" function before co-registration to the MRI images. Tumor findings were outlined in transverse slices, creating a volume of interest (VOI) around the tumor area. For the control group, the VOIs were outlined around the pituitary gland.

The VOIs in the postsurgical scans were created in the same manner as the presurgical VOIs, around areas of suspected residual tumor tissue or inconclusive abnormal findings in postoperative MRI scans. Tracer uptake was analyzed in the VOI with regard to maximum standardized uptake value (SUV_{max}). Data from the 35- to 45-minute frame was chosen for the statistical analysis. No measurements were performed for patients considered cured on the basis of combined biochemical and clinical factors and without any abnormal MRI findings.

2.6 | Tumor classification and immunohistochemical analyses

Tumor tissues samples were collected during surgery from the PitNET patients. Representative tumor tissue was confirmed in routine hematoxylin/eosin-stained sections

from formalin-fixed, paraffin-embedded tissue blocks. Pituitary tumors were classified into histological subtypes according to the 2017 WHO classification based on the immunohistochemical expression of anterior pituitary hormones (growth hormone [GH], TSH, prolactin [PRL], adrenocorticotrophic hormone [ACTH], luteinizing hormone [LH], and follicle-stimulating hormone [FSH]) and pituitary-specific transcription factors (T-Pit, SF-1, and Pit-1). Plurihormonal tumors were categorized as to their clinical presentation.

The following antibodies used were: anti-FSH (monoclonal, clone C10, DAKO, catalogue number M3504, dilution 1:300), anti-LH (monoclonal, clone 93C, DAKO, catalogue number M3502, dilution 1:400), anti-TSH (monoclonal, clone 0042, DAKO catalogue number M3503, dilution 1:100), anti-GH (polyclonal, catalogue number A0570, dilution 1:3000), anti-ACTH (monoclonal, clone 02A3, DAKO, catalogue number M3501, dilution 1:1200); anti-Pit-1 (Novus Biologicals, polyclonal, code no. NBP1-92273, dilution 1:500), anti-SF-1 (ThermoFisher Scientific, monoclonal, clone N1665, dilution 1:100) and anti-T-Pit (TBX19) (monoclonal, clone CL6251, Atlas Antibodies, dilution 1:1000). Normal pituitary gland served as a positive control for immunohistochemical analyses with the antibodies towards anterior pituitary hormones and pituitary-specific transcription factors. For each tumor, proliferation index Ki67 was analyzed (monoclonal antibody, clone MIB1, DAKO, catalogue number IR626/GA626, ready to use) and assessed by counting the percentage of Ki67 immunolabeled cells among 2000 tumor cells in hot spots regions. Normal lymph gland served as a positive control for Ki67 immunostaining. All immunohistochemical staining was performed with Dako EnVision FLEX system and DAKO Autostainer.

The immunohistochemical analyses of anterior pituitary hormones, pituitary-specific transcription factors, and SSTR were all performed with the same protocol, using specific monoclonal antibodies, as described in our previously published study.¹³ The immunoreactive score^{16,17} (IRS) was used for the quantification of SSTR expression, as the product of the proportion of immunoreactive cells (0 = 0%, 1 = <10%; 2 = 10-50%, 3 = 51-80%, and 4 = >80%) and the staining intensity (0 = no staining, 1 = weak; 2 = moderate, and 3 = strong). IRS-scoring was performed by an experienced pathologist (OC-B) who was blinded to the clinical data.

2.7 | Statistical analysis

All statistical analyses were performed using Prism 8.0 (GraphPad Software, Inc.). Normal distribution of data were tested with the Shapiro-Wilks test. Variables with continuous data are presented as means and standard deviations (SD), and variables not following normal distribution are presented as medians and interquartile ranges (IQR). Mann-Whitney U-test was used for comparison of ^{68}Ga -DOTATOC uptake in patients and controls. Spearman's rank-order correlation was used for correlation analyses between SSTR expression and SUV_{max} . For all tests, $P < .05$ was considered as statistically significant.

3 | RESULTS

3.1 | Preoperative ^{68}Ga -DOTATOC PET in patients and controls

Uptake data are presented as median (IQR) values. SUV_{max} was 15.9 (11.6-19.7), 6.8 (2.6-9.3), and 41.1 (37.4-60.0) for somatotroph, corticotroph, and thyrotroph tumors, respectively (Figure 1) [see Table 2 for individual values]. The median uptake in all 15 control subjects was SUV_{max} 13.8 (12.1-15.5). Compared to the normal pituitary gland, there was a significant difference in uptake in thyrotroph (Mann-Whitney $U = 0$; $P < .01$) and corticotroph tumors (Mann-Whitney $U = 11$; $P < .01$), but not for somatotroph tumors (Mann-Whitney $U = 42$; $P = .27$). Representative PET and MRI images along with corresponding immunohistochemical images of SSTR expression for each type tumor are presented in Figure 2A-C. In addition, dynamic data of tracer uptake in tumor subtypes and the normal pituitary gland are presented in Figure 4A and B. Dynamic data for gonadotroph tumors were also presented in a previous publication by the authors.¹³

3.2 | Postoperative ^{68}Ga -DOTATOC PET

Among the 20 patients who underwent postoperative PET scan, nine demonstrated unequivocal signs of complete tumor resection on postoperative MRI accompanied by corresponding clinical remission. The other 11 patients showed an abnormal postoperative MRI with findings of either a suspected residual tumor tissue or an inability to distinguish between scar tissue or residual tumor (Table 3). For tumors with preoperative uptake higher than the median uptake for controls ($\text{SUV}_{\text{max}} > 13.8$) a cut-off

level at 60% of the preoperative uptake could be observed, dividing the cured and non-cured patients. A low uptake postoperatively (<60% of the preoperative uptake) corresponded with clinical remission in all four cases. In these tumors with high uptake, a persistent SUV_{max} postoperatively representing >60% of the preoperative uptake corresponded with maintained hypersecretion in two cases. A figure illustrating these two groups can be found in the appendix.

3.3 | Histopathological characterization of PitNETs

In the eight patients with acromegaly, histopathological assessment demonstrated one pure somatotroph tumor, six somatolactotroph tumors, and one plurihormonal tumor with GH, PRL, TSH, FSH, and LH expression. Among patients with clinically thyrotroph tumors, one patient had a pure thyrotroph tumor and two patients had a plurihormonal tumors with GH, PRL, and TSH expression. Five patients with Cushing's disease and two patients with clinically NF-tumors had ACTH- and T-Pit-positive corticotroph tumors (Table 2).

TSH-producing tumors (two GH+PRL+TSH plurihormonal tumors and one pure thyrotroph tumor) expressed the highest degree of SSTR2 (median IRS 12) followed by moderately high expression of SSTR5 (median IRS 6) and SSTR3 (median IRS 6), but no expression of SSTR1 (median IRS 0).

In corticotroph tumors (silent corticotroph tumors included) there were low expression for SSTR1 and SSTR2 (median IRS 1 for SSTR1 and 2 for SSTR2), high expression of SSTR3 and SSTR5 (median IRS 12 for SSTR3 and SSTR5).

In patients with acromegaly (six somatolactotroph, one pure GH-producing and one plurihormonal tumor), SSTR expression was high for all receptors (median IRS 12 for SSTR2 and SSTR5, and 9 for SSTR3) except SSTR1 (median IRS 0) (Table 2).

3.4 | Correlation between $^{68}\text{Ga-DOTATOC}$ SUV_{max} and SSTR expression

Spearman's rank order correlation coefficient between SUV_{max} and SSTR expression was -0.31 for SSTR1 ($P = .23$), 0.75 for SSTR2 ($P < .01$), -0.37 for SSTR3 ($P = .14$), and -0.18 for SSTR5 ($P = 0.48$).

3.5 | Adverse events and incidental findings

Reported adverse events after PET scanning were headache, diarrhea, and nausea. There were no serious adverse events during the study. One patient (#10, Table 2) had an incidental finding of a dural mass located in the proximity of the left sigmoid and transverse dural venous sinuses with high ^{68}Ga -DOTATOC uptake (SUV_{max} 26) (Figure 2A). Further clinical investigation later confirmed a meningioma.

4 | DISCUSSION

This pilot study evaluated the diagnostic properties of the ^{68}Ga -DOTATOC tracer for hormone-secreting PitNETs with respect to their histopathological features and demonstrates its clinical value in pre- and postoperative imaging of thyrotroph tumors. SUV_{max} correlated with SSTR2 expression intensity, which was expressed to the highest degree in both thyrotroph (both pure TSH-producing and plurihormonal tumors) and somatotroph tumors. The study also found significant differences in tracer uptake between the normal pituitary gland and both thyrotroph and corticotroph tumors. This observation is of high clinical relevance as the diagnostic procedure of thyrotroph tumors is complex and time consuming. The process for confirmation of a thyrotroph tumor is based on proving autonomous TSH production through extensive endocrine testing,¹⁸ as NF-PitNETs are much more common than TSH-producing tumors.¹⁹ NF-PitNETs were previously demonstrated to have a significantly lower uptake of ^{68}Ga -DOTATOC compared to the normal pituitary gland in our previous study.¹³ Therefore, the tracer adds valuable information in that it may distinguish thyrotroph tumors from both NF-PitNETs and the normal pituitary gland.

In somatotroph tumors, SSTR2 and SSTR5 receptors were expressed to the highest degree (median IRS 12 for both), but with a similar tracer uptake to normal pituitary tissue (mean SUV_{max} 15.5 compared to 13.8 in normal pituitary gland). Interestingly, somatotroph tumors showed significantly lower tracer uptake compared to thyrotroph tumors despite both groups demonstrated equally high SSTR2 expression (median IRS of 12 for both groups). In contrast to thyrotroph tumors, somatotroph tumors demonstrated much higher expression of both SSTR3 and SSTR5, which paradoxically

rendered a lower tracer uptake value. One hypothesis that could be derived from this is that a higher total number of receptors induce competitive interference at the receptor level, which results in a lower overall tracer uptake. Another explanation could be that the IRS scale is an ordinal scale and based on visual, semi-quantitative determination. Thereby, there could still be a numerical difference in number of receptors between these tumors, even though both showed a visually determined IRS score of 12.

On the contrary to thyrotroph and somatotroph tumors, tracer uptake in corticotroph tumors was generally lower in the tumor region compared to normal pituitary tissue (Figures 1 and 2B). This is in line with a previous study that evaluated smaller corticotroph tumors with ^{68}Ga -DOTATATE, demonstrating a significant lower tracer uptake in these tumors (mean SUV_{max} 3.5 ± 2.1 in tumors compared to 5.9 ± 2.7 in normal pituitary tissue, $P < .01$).¹⁴ Interestingly, we found higher median uptake in these tumors using ^{68}Ga -DOTATOC compared to the above mentioned study using ^{68}Ga -DOTATATE,¹⁴ even though DOTATATE demonstrates higher affinity to the SSTR2 receptor.²⁰ Further comparison is however precarious, since other methodological differences also may contribute. Even though both studies found significantly lower uptake in corticotroph tumors, the clinical significance is nonetheless limited, especially in the postoperative image assessment, as the lower uptake could not be inferred as a tumor-specific finding.

In total, three tumors demonstrated immunohistochemical expression of multiple hormones belonging to the Pit-1 cell lineage. According to the modified WHO 2017 classification of pituitary tumors, plurihormonal tumors are considered to be a distinct subgroup of tumors within the Pit-1-positive cell lineage apart from lactotroph, somatotroph, and thyrotroph tumor groups.²¹ However, in this study, they were classified according to their clinical presentation as in clinical practice, with two patients in the TSH-hypersecretion group and one patient in the acromegaly group (Figure 1 and Table 2). These plurihormonal tumors demonstrated no significant difference in uptake from the pure TSH-producing and somatolactotroph tumors and could not be considered as outliers in their group.

^{68}Ga -DOTATOC PET added limited value to the postsurgical evaluation generally. Only thyrotroph tumors demonstrated a significantly higher tumor uptake than the pituitary gland, distinguishing them from both scar tissue and normal pituitary tissue in the

postoperative image assessment. As an illustrative case, one patient who presented with a thyrotroph tumor had an inconclusive abnormal MRI finding postoperatively. The tracer showed low uptake in the abnormal MRI finding, which corresponded with scar tissue (Figure 3). For the other tumors, there were no significant differences in uptake compared to the pituitary gland or high enough to be regarded as a tumor-specific finding. However, when comparing uptake levels between the pre- and postoperative PET in the same patients, tracer uptake level at 60% was observed to distinguish clinical and biochemical remission from non-cure for tumors with a preoperative uptake above the median uptake of the normal pituitary (SUV_{max} 13.8). For patients with a preoperative uptake $SUV_{max} >13.8$ but with a postoperative uptake $SUV_{max} <60\%$ of the preoperative uptake, the tracer correctly identified clinical remission in all cases and, conversely, patients with no biochemical remission demonstrated a postoperative $SUV_{max} >60\%$ in both cases (Table 3).

As a major strength of this study, uptake data of the different subgroups of PitNETs were accompanied by histopathological data on adenohypophyseal cell types based on both transcription factors and staining for adenohypophyseal hormones. Also, the degree of SSTR expression has been presented in a quantitative scale that provides a more detailed description of tumor heterogeneity regarding tracer uptake. We found a significant correlation between tracer uptake and the expression of the SSTR2 receptor, evoking the hypothesis that medical treatment with somatostatin analogues could be monitored in tumors with excessive SSTR2 expression, i.e. in thyrotroph tumors. Analogously, tumors with high degree of SSTR3 expression, i.e. corticotroph and gonadotroph tumors, may be better detected and monitored by tracers such as DOTANOC, with high affinity to this receptor. This may be within the scope for future studies.

The major limitation of our study was the small number of cases, a consequence of studying rare tumors. Although this study suggests a potential role of the ^{68}Ga -DOTATOC tracer in pre- and postoperative image assessment in thyrotroph tumors, the limited number of patients still makes these results somewhat uncertain and further evaluation in larger cohorts is needed to confirm this. Uptake differences in somatotroph tumors and normal pituitary tissue were indicated in this study, but could not be proven with statistical significance, presumably because of the small sample size. For smaller

tumors, there are several methodological limitations by using ^{68}Ga -DOTATOC. First, the relatively high positron energy for ^{68}Ga (mean $E_{\text{mean}} = 0.83$ MeV) needs to be considered, which yields a long positron range of $R_{\text{mean}} = 3.5$ mm,²² resulting in a limited intrinsic image resolution. Furthermore, the partial-volume effect displays a confounding factor for tracer uptake, especially in assessing smaller tumors and smaller postoperative findings. SUVmax may be impacted by several other factors than SSTR expression such as partial volume effect that, in turn, may be influenced by both size of the lesion as well as movements of the subjects. However, since validated methods for partial volume correction in PitNETs have not been published, no adjustments for this potential effect was performed. Instead, we present unmodified uptake data as it was measured, with a caveat of possible significant impact of partial volume effect in smaller lesion, in particular lesion under 1 centimeter. Also, the postoperative PET evaluations were relatively few, as postoperative evaluations had to be delayed because of the current Covid-19 pandemic.

However, even as a small pilot study, this study demonstrated a significant difference in uptake levels between thyrotroph and corticotroph tumors versus normal pituitary tissue and interesting postoperative results that cured patients may be discriminated from non-cured patients based on PET uptake if tumors preoperatively presented with a high uptake. This study also presents interesting findings regarding SSTR expression in PitNETs, in particular the high SSTR3 expression in both corticotroph tumors, that could be the starting point for further, more focused studies.

REFERENCES

1. Asa SL, Casar-Borota O, Chanson P, et al. From pituitary adenoma to pituitary neuroendocrine tumor (PitNET): an International Pituitary Pathology Club proposal. *Endocr Related Cancer*. 2017;24(4):C5-C8.
2. Lloyd R, Osamura R, Kloppel G, Rosai J, eds. *WHO Classification of Tumours of Endocrine Organs*. 4th edition, volume 10. Lyon, France: International Agency for Research on Cancer (IARC); 2017.
3. Chanson P, Salenave S. Diagnosis and treatment of pituitary adenomas. *Minerva Endocrinol*. 2004;29(4):241-275.
4. Monson JP. The epidemiology of endocrine tumours. *Endocr Relat Cancer*. 2000;7(1):29-36.
5. Asa SL, Ezzat S. The cytogenesis and pathogenesis of pituitary adenomas. *Endocr Rev*. 1998;19(6):798-827.
6. Pinker K, Ba-Ssalamah A, Wolfsberger S, Mlynarik V, Knosp E, Trattnig S. The value of high-field MRI (3T) in the assessment of sellar lesions. *Eur J Radiol*. 2005;54(3):327-334.
7. Tabarin A, Laurent F, Catargi B, et al. Comparative evaluation of conventional and dynamic magnetic resonance imaging of the pituitary gland for the diagnosis of Cushing's disease. *Clin Endocrinol (Oxf)*. 1998;49(3):293-300.
8. Chittiboina P, Montgomery BK, Millo C, Herscovitch P, Lonser RR. High-resolution ^{18}F -fluorodeoxyglucose positron emission tomography and magnetic resonance imaging for pituitary adenoma detection in Cushing disease. *J Neurosurg*. 2015;122(4):791-797.
9. Escourolle H, Abecassis JP, Bertagna X, et al. Comparison of computerized tomography and magnetic resonance imaging for the examination of the pituitary gland in patients with Cushing's disease. *Clin Endocrinol (Oxf)*. 1993;39(3):307-313.
10. Frilling A, Sotiropoulos GC, Radtke A, et al. The impact of ^{68}Ga -DOTATOC positron emission tomography/computed tomography on the multimodal management of patients with neuroendocrine tumors. *Ann Surg*. 2010;252(5):850-856.

11. Gabriel M, Decristoforo C, Kendler D, et al. ^{68}Ga -DOTA-Tyr3-octreotide PET in neuroendocrine tumors: comparison with somatostatin receptor scintigraphy and CT. *J Nucl Med*. 2007;48(4):508-518.
12. Sundin A, Arnold R, Baudin E, et al. ENETS consensus guidelines for the standards of care in neuroendocrine tumors: radiological, nuclear medicine & hybrid imaging. *Neuroendocrinology*. 2017;105(3):212-244.
13. Tjörnstrand A, Casar-Borota O, Heurling K, et al. Lower ^{68}Ga -DOTATOC uptake in nonfunctioning pituitary neuroendocrine tumours compared to normal pituitary gland – a proof-of-concept study. *Clin Endocrinol (Oxf)*. 2020;92(3):222-231.
14. Wang H, Hou B, Lu L, et al. PET/MRI in the diagnosis of hormone-producing pituitary microadenoma: a prospective pilot study. *J Nucl Med*. 2018;59(3):523-528.
15. Lastoria S, Marciello F, Faggiano A, et al. Role of ^{68}Ga -DOTATATE PET/CT in patients with multiple endocrine neoplasia type 1 (MEN1). *Endocrine*. 2016;52(3):488-494.
16. Remmele W, Stegner HE. Recommendation for uniform definition of an immunoreactive score (IRS) for immunohistochemical estrogen receptor detection (ER-ICA) in breast cancer tissue. *Pathologe*. 1987;8(3):138-140.
17. Casar-Borota O, Heck A, Schulz S, et al. Expression of SSTR2a, but not of SSTRs 1, 3, or 5 in somatotroph adenomas assessed by monoclonal antibodies was reduced by octreotide and correlated with the acute and long-term effects of octreotide. *J Clin Endocrinol Metab*. 2013;98(11):E1730-1739.
18. Tjörnstrand A, Nyström HF. Diagnostic approach to TSH-producing pituitary adenoma. *Eur J Endocrinol*. 2017;177(4):R183-197.
19. Tjörnstrand A, Gunnarsson K, Evert M, et al. The incidence rate of pituitary adenomas in western Sweden for the period 2001-2011. *Eur J Endocrinol*. 2014;171(4):519-526.
20. Reubi JC, Schar JC, Waser B, et al. Affinity profiles for human somatostatin receptor subtypes SST1-SST5 of somatostatin radiotracers selected for scintigraphic and radiotherapeutic use. *Eur J Nucl Med*. 2000;27(3):273-282.
21. Lopes MBS. The 2017 World Health Organization classification of tumors of the pituitary gland: a summary. *Acta Neuropathol*. 2017;134(4):521-535.

22. Conti M, Eriksson L. Physics of pure and non-pure positron emitters for PET: a review and a discussion. *EJNMMI Phys.* 2016;3(1):8.

Accepted Article

TABLE 1 Baseline data for the clinical presentation of 18 pituitary tumor patients undergoing ^{68}Ga -DOTATOC PET before endoscopic pituitary surgery

Patient no.	MRI tumor size (mm)^a	Age (years)	Gender	Body weight (kg)	^{68}Ga-DOTATOC dose (MBq)
#1 ^b	16 × 17 × 19	44	F	65	162.0
#2 ^b	25 × 27 × 37	51	M	87	177.0
#3	22 × 21 × 16	35	F	76	135.0
#4	12 × 13 × 15	43	M	116	240.0
#5	12 × 9 × 10	34	M	88	170.3
#6	14 × 16 × 19	47	M	86	172.0
#7	12 × 11 × 10	61	F	93.2	191.0
#8	11 × 10 × 9	64	M	100	200.0
#9	8 × 3 × 3	74	M	92	188.1
#10	10 × 20 × 10	45	M	128	261.0
#11	5 × 5 × 5	52	F	86	178.0
#12	3 × 3 × 3	43	F	71.4	139.0
#13	11 × 14 × 7	37	F	63	129.5

#14	3 × 3 × 4	51	F	66	132.0
#15	4 × 4 × 4	20	M	88	176.0
#16	20 × 20 × 20	62	F	72	150.0
#17	5 × 5 × 5	25	F	86	175.4
#18	16 × 18 × 19	33	M	100	213.0

Abbreviations: F, female; M, male; MRI, magnetic resonance imaging; PET, positron emission tomography.

^aLength, width, and height dimensions, respectively.

^bPublished previously.¹³

TABLE 2 Presenting information from preoperative ^{68}Ga -DOTATOC PET and histopathological data for tumor specimens that were removed during endoscopic surgery of 18 patients with pituitary neuroendocrine tumors. Data are presented according to histopathological staining of adenohypophyseal hormones. Individual values are presented as SUV_{max} and IRS. For group data SUV_{max} and IRS data are presented as the median value for each group

Patient	Clinical presentation	Tumor type ^a	$\text{SUV}_{\text{max}}^{\text{b}}$	IRS ^c			
				SSTR1	SSTR2	SSTR3	SSTR5
PitNET		Corticotroph	6.8	1	2	12	12
#1 ^d	Pituitary insufficiency	ACTH	4.1	2 × 3 = 6	0 × 0 = 0	3 × 2 = 6	0 × 0 = 0
#2 ^d	Pituitary insufficiency	ACTH	1.3	0 × 0 = 0	0 × 0 = 0	4 × 3 = 12	2 × 2 = 4
#11	Cushing's disease	ACTH	2.6	1 × 2 = 2	2 × 3 = 6	3 × 2 = 6	4 × 3 = 12
#12	Cushing's disease	ACTH	9.3	1 × 3 = 3	2 × 3 = 6	4 × 3 = 12	4 × 3 = 12
#13	Cushing's disease	ACTH	7.3	0 × 0 = 0	1 × 2 = 2	4 × 3 = 12	4 × 3 = 12
#14	Cushing's disease	ACTH	6.8	0 × 0 = 0	1 × 2 = 2	4 × 3 = 12	4 × 3 = 12
#15	Cushing's disease	ACTH	14.6	1 × 1 = 1	1 × 3 = 3	4 × 3 = 12	4 × 3 = 12
PitNET		Somatotroph	15.9	0	12	9	12
#3	Acromegaly	GH+PRL	10.9	0 × 0 = 0	3 × 3 = 9	3 × 2 = 6	1 × 1 = 1
#4	Acromegaly	GH+PRL	14.7	0 × 0 = 0	4 × 3 = 12	3 × 3 = 9	4 × 3 = 12
#5	Acromegaly	GH+PRL	17.4	1 × 1 = 1	3 × 1 = 3	4 × 3 = 12	4 × 3 = 12

#6	Acromegaly	GH+PRL	7.7	0 × 0 = 0	4 × 3 = 12	3 × 3 = 9	4 × 3 = 12
#7	Acromegaly	GH+PRL	15.5	1 × 1 = 1	4 × 3 = 12	2 × 3 = 6	3 × 3 = 9
#8	Acromegaly	GH+PRL	16.2	0 × 0 = 0	4 × 3 = 12	3 × 3 = 9	4 × 3 = 12
#9	Acromegaly	GH+PR+TSH+FSH+LH	21.1	0 × 0 = 0	4 × 3 = 12	3 × 2 = 6	1 × 2 = 2
#10	Acromegaly	GH	20.5	– ^e	4 × 3 = 12	– ^e	3 × 3 = 9
PitNET		Thyrotroph	41.1	0	12	6	6
#16	TSH hypersecretion	TSH+GH+PRL	37.4	0 × 0 = 0	4 × 3 = 12	2 × 3 = 6	2 × 3 = 6
#17	TSH hypersecretion	TSH	41.1	0 × 0 = 0	4 × 3 = 12	1 × 2 = 2	1 × 1 = 1
#18	TSH hypersecretion	TSH+GH+PRL	60.0	0 × 0 = 0	4 × 3 = 12	3 × 3 = 9	4 × 3 = 12

Abbreviations: ACTH, adenocorticotrophic hormone; GH, growth hormone; IHC, immunohistochemistry, IRS, immunoreactive score; PET, positron emission tomography; PRL, prolactin; SSTR, somatostatin receptor; SUV_{max}, maximum standardized uptake value.

^aDetermined by immunohistochemistry with monoclonal antibodies towards adenohipophyseal hormones and tumor-specific transcription factors.

^bPET data from the region of interest containing the tumor with SUV_{max} measured over the 35- to 45-minute frame.

^cIRS determined as the product of the proportion of immunoreactive cells (0 = 0%, 1 = <10%; 2 = 10-50%, 3 = 51-80%, and 4 = >80%) and the staining intensity (0 = no staining, 1 = weak; 2 = moderate, and 3 = strong). Group data presented as median IRS value.

^dPublished previously.¹³

^eNo histopathological data.

TABLE 3 Pre- and postoperative ^{68}Ga -DOTATOC PET data and postoperative MRI findings in 11 patients with pituitary tumors where the postoperative MRI was inconclusive

Patient no.	Cell type	Clinically cured ^a	Postoperative	MRI interpretation	Preoperative	Postoperative	PET2/PET1
			MRI tumor size (mm) ^b		SUV _{max} (PET1)	SUV _{max} (PET2)	SUV _{max} ratio (%)
#1 ^c	Corticotroph	Yes	8 × 3 × 3	Inconclusive	4.1	4.2	102
#2 ^c	Corticotroph	No	3 × 4 × 4	Tumor likely	1.3	4.6	308
#3	Somatotroph	No	12 × 7 × 18	Tumor likely	10.9	4.6	42
#4	Somatotroph	Yes	4 × 3 × 4	Inconclusive	14.0	7.1	51
#6	Somatotroph	Yes	2.5 × 3 × 3	Inconclusive	7.7	7.3	95
#7	Somatotroph	No	7 × 7 × 7	Tumor likely	15.5	11.0	71
#8	Somatotroph	Yes	5 × 5 × 5	Tumor likely	16.2	4.7	29
#18	Thyrotroph	Yes	5 × 3 × 5	Inconclusive	60.0	6.0	10
#21 ^c	Gonadotroph	No	20 × 20 × 20	Tumor likely	14.4	15.3	106
#22 ^c	Gonadotroph	Yes	3 × 4 × 3	Inconclusive	16.6	5.2	31
#24 ^c	Gonadotroph	No	2 × 3 × 2	Tumor likely	3.3	4.8	145

Abbreviations: MRI, magnetic resonance imaging; PET, positron emission tomography; SUV_{max}, maximum standardized uptake value.

^aOn the basis of clinical and biochemical factors.

^bLength, width, and height dimensions, respectively.

^cPublished previously.¹³

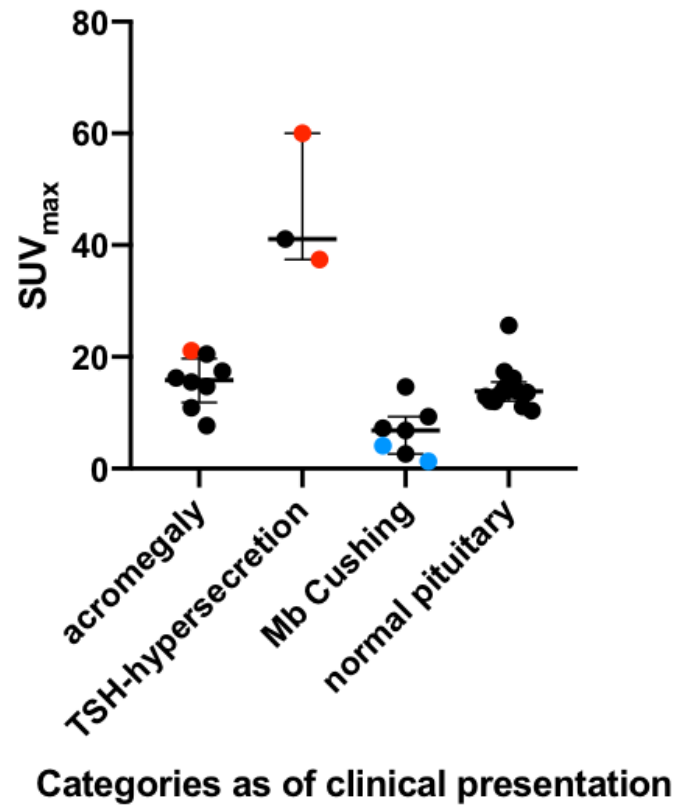
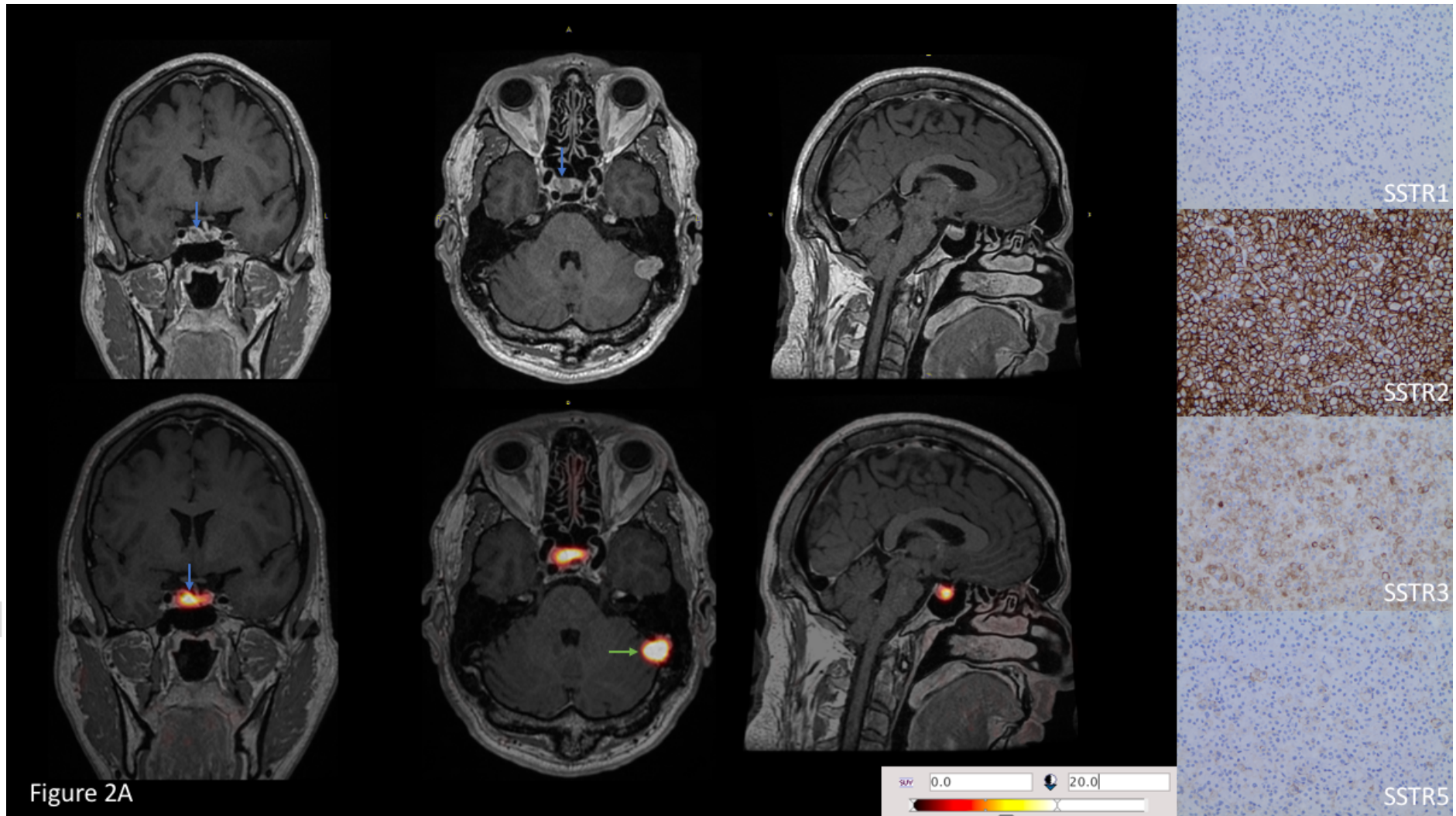
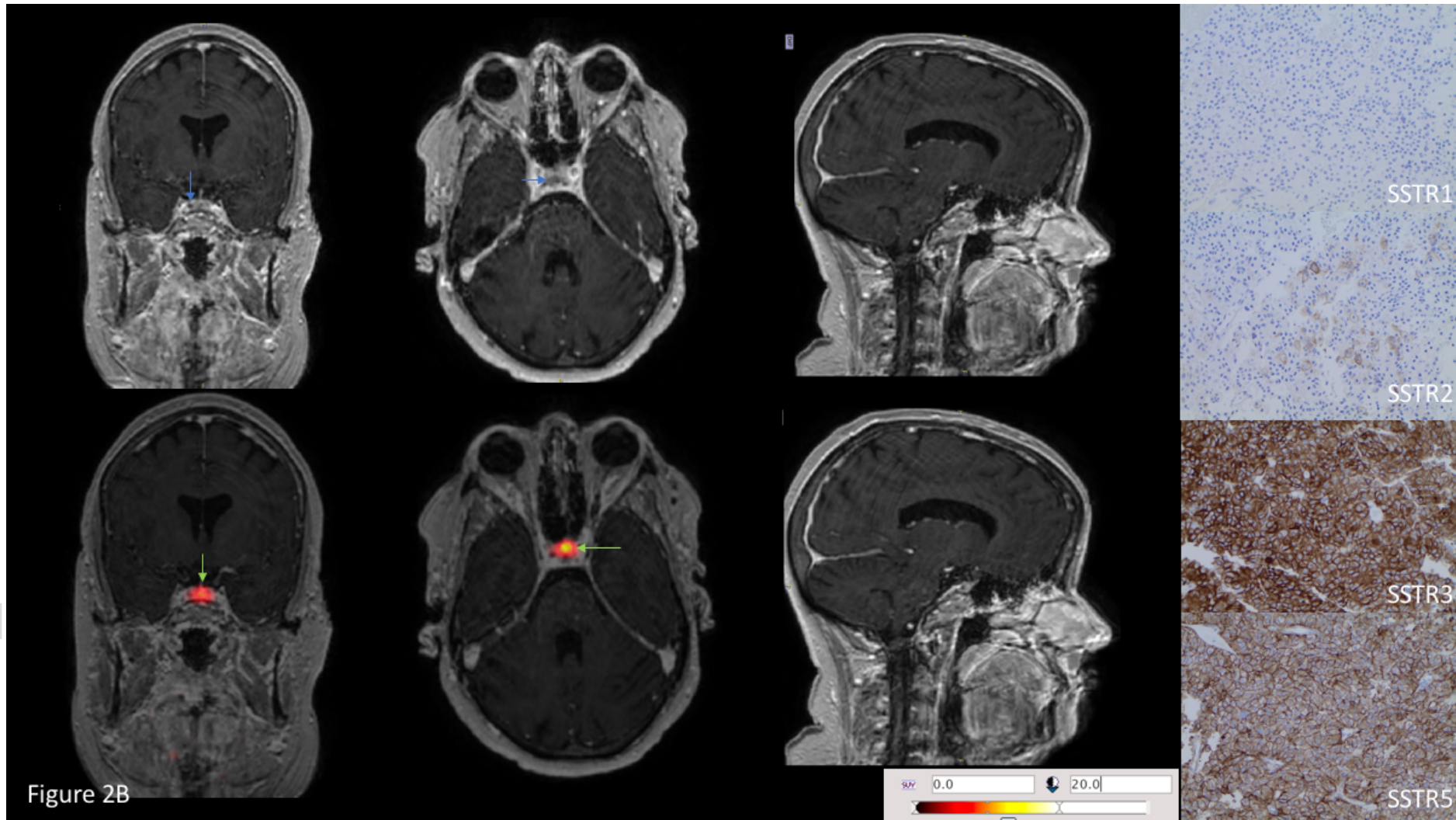
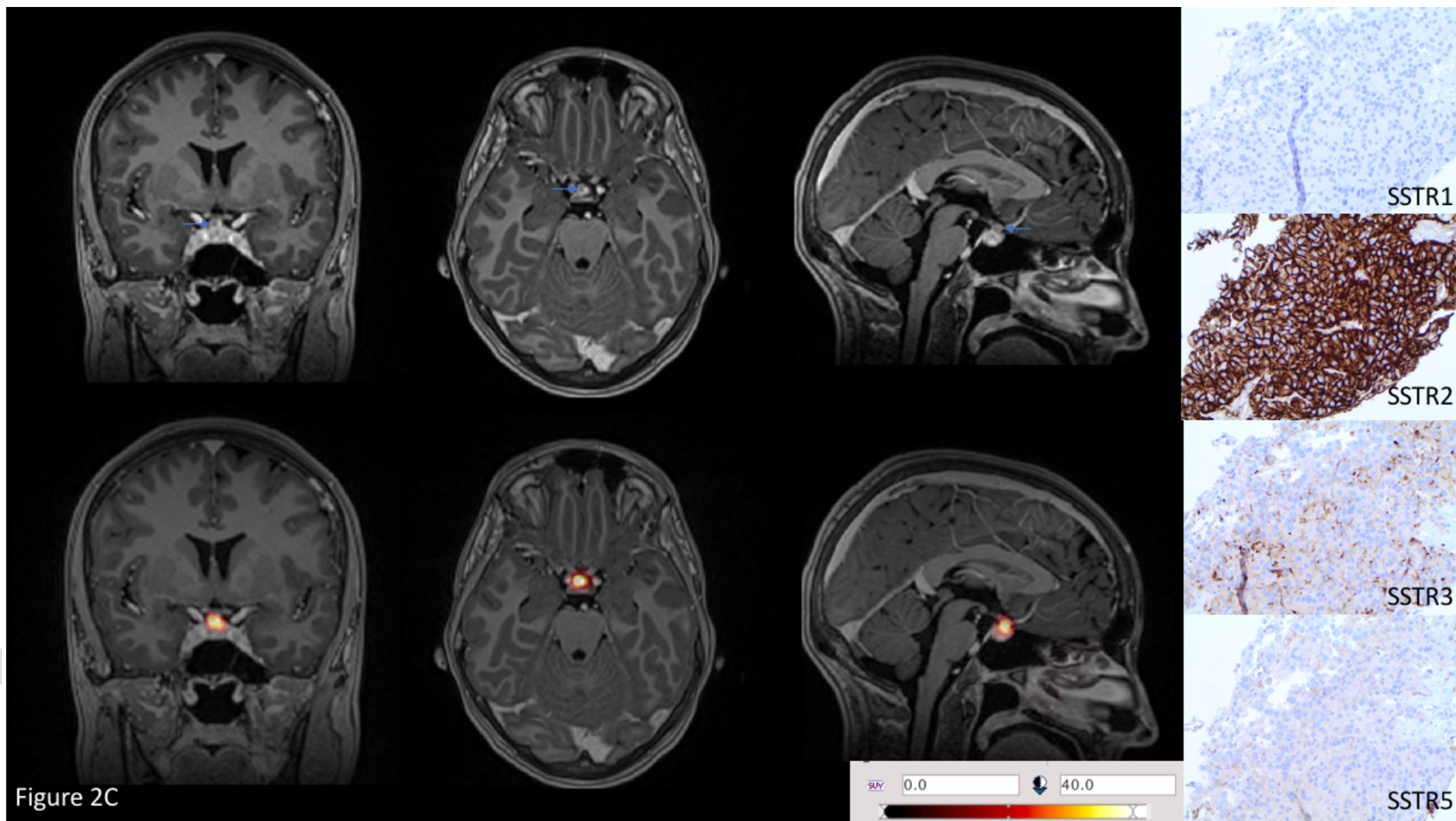
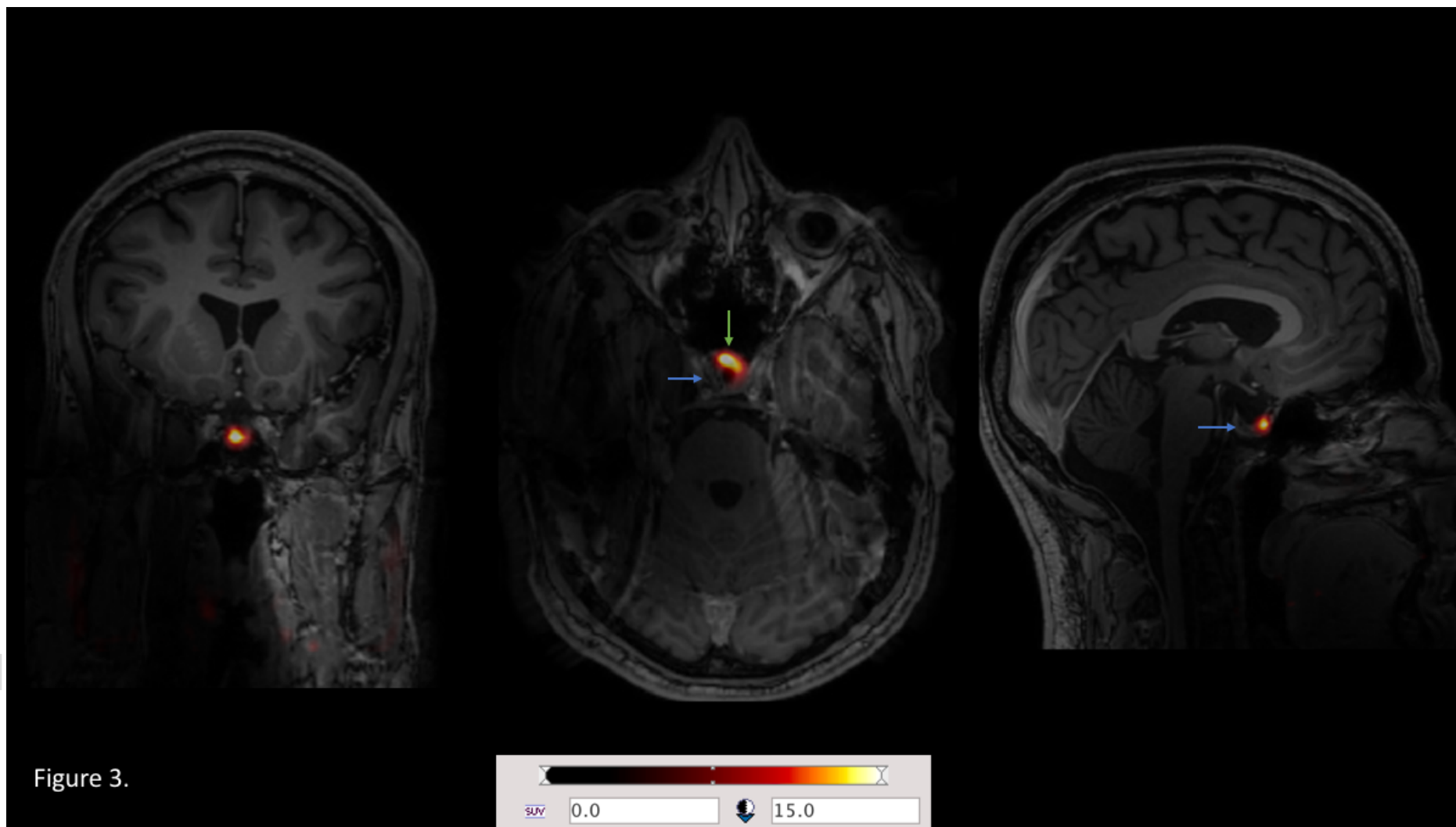


Figure 1.









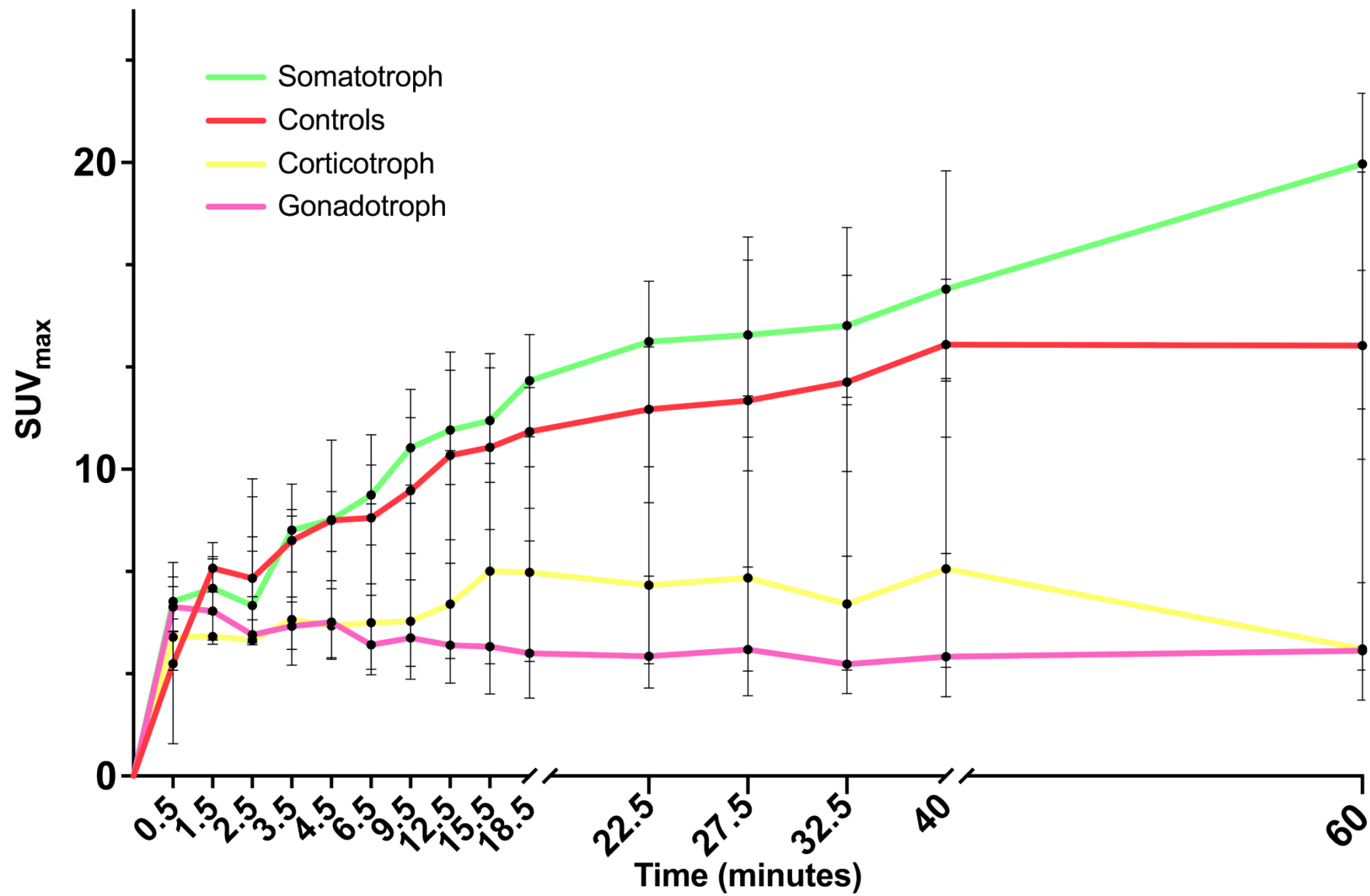


Figure 4A.

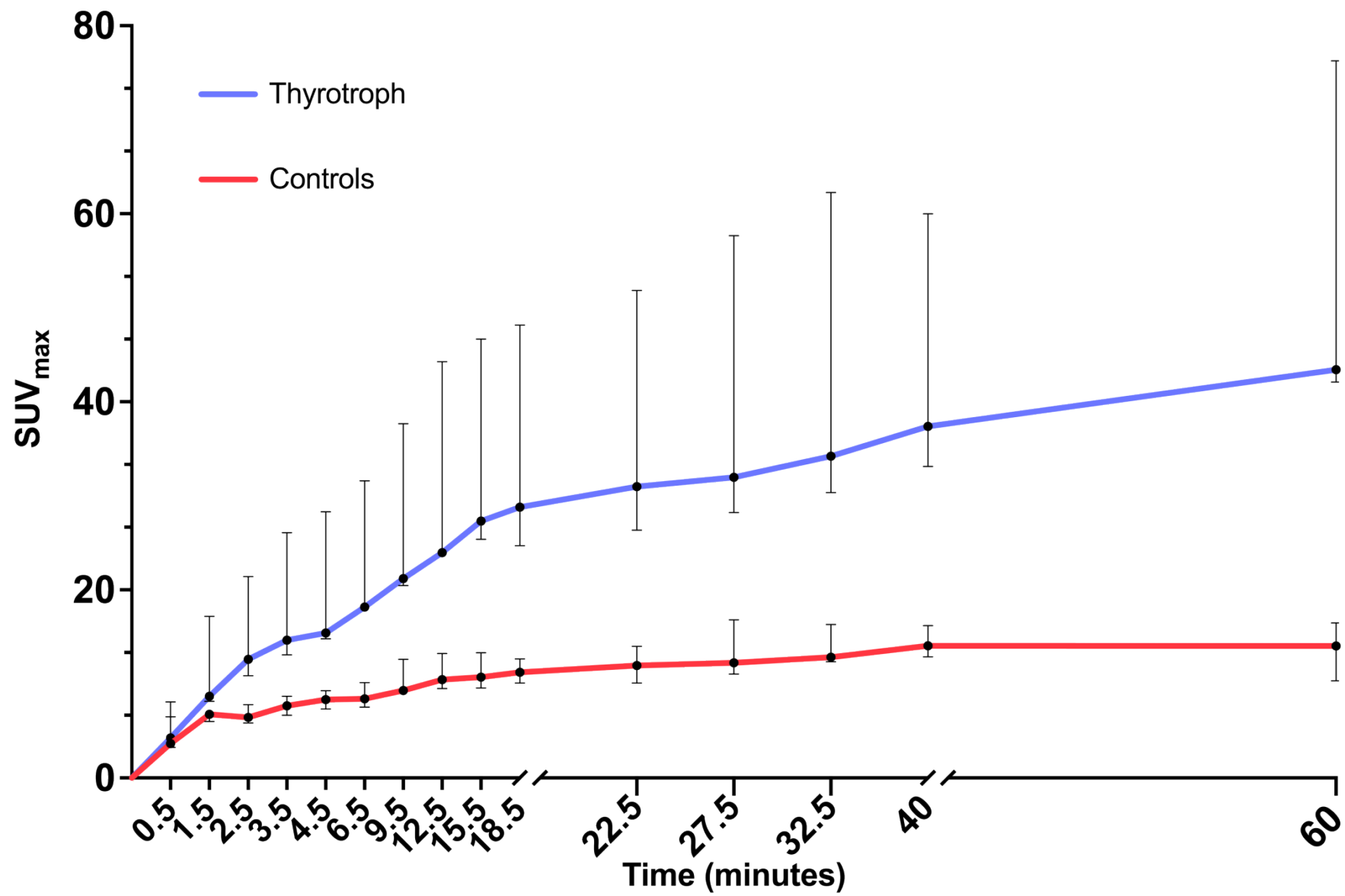


Figure 4B.

s protected by copyright. All rights reserved

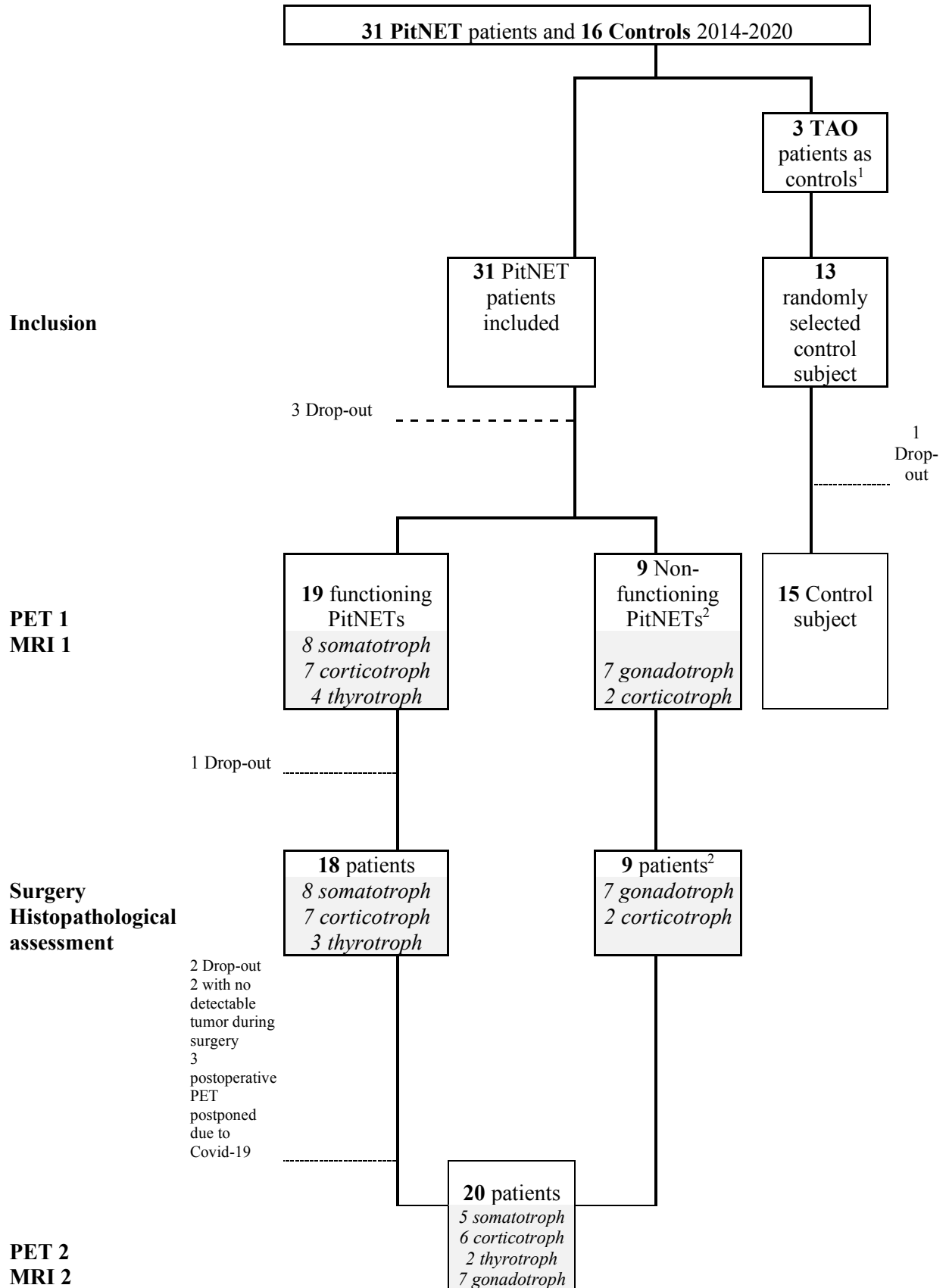
FIGURE LEGENDS

FIGURE 1 Scatterplot of SUV_{max} from the 35-45 minute frame for the 18 patients with different pituitary tumor categories at clinical presentation and 15 control subjects with normal pituitary. Individual dots represent plurihormonal tumors (red) and non-functioning tumors with silent corticotroph origin (blue). Two corticotroph tumors and controls #1-13 have been presented in a previous publication¹³

FIGURE 2 Preoperative images demonstrating MRI alone and co-registered PET and MRI images plus immunohistochemical images of SSTR expression for three patients. **A.** Patient with a $10 \times 20 \times 10$ mm large somatotroph pituitary tumor (blue arrow). There is incidental uptake in a dural mass in the left sigmoid sinus that was later diagnosed as a meningioma (green arrow). SSTR expression showed IRS 0, 12, 6, and 2 for SSTR1, SSTR2, SSTR3, and SSTR5, respectively. **B.** Patient with a $3 \times 3 \times 4$ mm small corticotroph tumor (blue arrow). There is evidently higher uptake in the normal pituitary to the left in the sella (green arrow) than in the tumor to the right (blue arrow). SSTR expression showed IRS 0, 2, 12, and 12 for SSTR1, SSTR2, SSTR3, and SSTR5, respectively. The MRI images are affected with imaging artifacts. **C.** Patient with a $5 \times 5 \times 5$ mm large thyrotroph tumor located in the superior part of the sella, paramedially to the right, in close proximity to the pituitary stalk (blue arrow). The scale is adjusted up SUV_{max} 40 because of high uptake. SSTR expression showed IRS 0, 12, 2, and 1 for SSTR1, SSTR2, SSTR3, and SSTR5, respectively

FIGURE 3 Postoperative PET-MRI images for a patient with a thyrotroph tumor. MRI revealed an abnormal finding in the inferior right of the sella, which was inconclusive to determine residual tumor or scar tissue (blue arrow). Preoperative tumor uptake was SUV_{max} 60. The abnormal finding in the postoperative MRI demonstrated an uptake of SUV_{max} 6. In the anterior and left part of the sella, there is a homogenous uptake of SUV_{max} 15, corresponding to normal pituitary gland (green arrow). The images are affected by dimming artifacts in the right part of the neck.

Figure 4 Demonstrating the uptake levels of ^{68}Ga -DOTATOC in different PitNETs subtypes and control subjects over time. SUV_{max} value on the Y-axis and time in minutes in the X-axis. Error bars show interquartile ranges. **A.** Figure illustrating the uptake from somatotroph, corticotroph and gonadotroph tumors as well as the uptake in the healthy normal pituitary gland. **B.** Figure showing the uptake in thyrotroph tumors and normal pituitary gland. The Y-axis range up to SUV_{max} 80 in this graph.



1 = control subject also part of a TAO study (<http://www.clinicaltrials.gov>; identifier NCT02378298)

2 = preoperative data presented in a previous study. DOI: 10.1111/cen.14144

Figure legend postoperative patients.

Figure demonstrating post-operative uptake profiles for six patients with a pre-operative tumor uptake of $SUV_{max} > 13.8$. Four patients with a post-operative uptake with $< 60\%$ of pre-operative uptake corresponded with biochemical cure. Conversely, in two patients with tumor uptake $> 60\%$ of the pre-operative uptake, the uptake corresponded with a persistent tumor